Renewable and Sustainable Energy Reviews 37 (2014) 397–407

Contents lists available at ScienceDirect

Renewable and Sustainable Energy Reviews

journal homepage: www.elsevier.com/locate/rser

A review of semiconductor materials as sensitizers for quantum dot-sensitized solar cells

M. Kouhnavard [a], S. Ikeda [a], N.A. Ludin [b,*], N.B. Ahmad Khairudin [a], B.V. Ghaffari [a], M.A. Mat-Teridi [b], M.A. Ibrahim [b], S. Sepeai [b], K. Sopian [b]

[a] Malaysia–Japan International Institute of Technology, Universiti Teknologi Malaysia, Kuala Lumpur 54100, Malaysia
[b] Solar Energy Research Institute, Universiti Kebangsaan Malaysia, Bangi 43600, Selangor, Malaysia

ARTICLE INFO

Article history:
Received 14 June 2013
Received in revised form
14 April 2014
Accepted 10 May 2014
Available online 3 June 2014

Keywords:
Quantum dot sensitized solar cell (QDSSC)
Sensitizer
Power conversion efficiency
QDs

ABSTRACT

Quantum dot-sensitized solar cells (QDSSCs) are renowned energy devices known for their distinct qualities, including (i) the ability to harvest sunlight that generates multiple electron–hole pairs, (ii) simplicity in fabrication, and (iii) low cost. The power conversion efficiency (η) rates of many QDSSCs are lower than those of dye-sensitized solar cells, reaching a maximum of 12% as a result of narrow absorption ranges and of the charge recombination occurring at the QD– and TiO_2–electrolyte interfaces. New types of sensitizers are necessary to be developed to further increase the η of QDSSCs. Semiconductor QDs are the most applicable material for photosensitization because of their high absorption and the obtained emission spectra that can be manipulated by varying dot sizes.

This paper presents an overview of recent studies on QDSSC photosensitization and provides suggestions to improve QDSSCs by explicitly comparing different sensitizers. Particular focus is directed on the behavior of several important types of semiconductor nanomaterials (sensitizers such as CdS, Ag_2S, CdSe, CdTe, CdHgTe, InAs, and PbS) and other nanomaterials that are TiO_2, ZnO, and carbon-based species. These materials are developed to enhance the electron transfer efficiency of QDSSCs. Understanding the mechanism of various photosensitization processes can provide design guidelines for future successful applications.

Contents

* Corresponding author. Tel.: +60 389118586; fax: +60 3 89118574.
E-mail address: sheekeen@ukm.edu.my (N.A. Ludin).

http://dx.doi.org/10.1016/j.rser.2014.05.023
1364-0321/

1. Introduction

The emergence of global warming and its associated climate change due to excessive use of fossil fuels has led us to focus on renewable energy sources for the future [1,2]. Several renewable energy sources are being investigated to evaluate their potential to address large-scale demand. These sources include wind turbines, hydropower, wave and tidal power, solar cells, solar thermal, and so on. Among these sources, photovoltaic (PV) technology, which utilizes solar energy, has drawn great attention as a solution to the increasing energy demand [3–5]. The sun provides a considerable amount of energy for our planet; the energy provided by the sun is approximately 10,000 times more than the global demand (i.e., 3×10^{24} J/year). In other words, covering 0.1% of the earth's surface with solar cells that have an efficiency of 10% would fulfill our present needs [6].

The PV market has shown exponential growth considering the technological and economic advances over the last few years. PV cells are commonly classified as first-, second-, and third-generation devices depending on the underlying technology. First-generation solar cells based on single- or multi-crystalline p–n junction silicon cells are the most common PV converters; these cells have a current market share of approximately 85%. Silicon-based PV devices have reached the power conversion efficiency of over 20% [7]. However, high purity requirements for silicon crystals, high fabrication temperatures, high material cost, and negative environmental impact of the processing technologies are major problems that should be resolved [8].

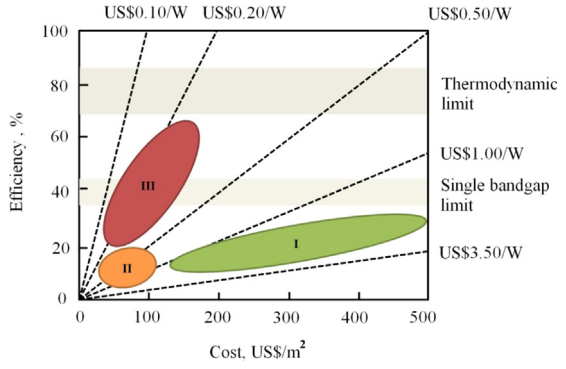

Fig. 1. Efficiency and cost projection for first (I), second (II), and third generation (III) photovoltaic technology [10].

Second-generation PV devices based on inorganic thin films have a current market share of approximately 15%; these devices are mostly based on CdTe. Second-generation PV devices are cheaper but are less efficient (14%) than first-generation single-junction crystalline PV cells (approximately 33%) [9]. Thus, for further improvement, a new technology is required to produce third-generation solar cells with an efficiency of more than 33% and has lower production cost.

Implementing these new concepts would make PV the cheapest option for future energy production. Fig. 1 shows the PV production cost per square meter with solar cell efficiency and the cost per unit power for the three generations of the technology [10]. First-generation wafer technology is identified by high production costs and has an average efficiency of 20%. Second-generation thin film technology offers lower production costs and moderate efficiency (presently $5 \pm 10\%$). High-efficiency devices with low production costs are possible with the exposure and advancement of third-generation solar cells, such as dye-sensitized solar cells (DSSCs), quantum dot-sensitized solar cells (QDSSCs), and organic solar cells.

The production cost for glass-based DSSCs with current techniques and materials is approximately between \$150 and \$220/m^2 [11,12]. With a module efficiency of approximately 5–8%, glass-based DSSCs cost approximately \$3/Wp to \$4/Wp [11,12], which is relatively higher than the approximately \$3/Wp of silicon-based PV modules [12]. The costs of glass-based DSSCs are expected to decrease to approximately \$1.4/Wp in the near future as the DSSC technology matures for high volume production [11]. DSSCs are considered low-cost and high-efficiency solar cells because their manufacture requires low-cost materials and simple processes with added functionalities, such as low weight, flexibility, and semi-transparency. Since Grätzel and O'Regan fabricated DSSCs in 1991 [13], extensive efforts have been exerted to increase the efficiency of DSSCs. However, the development of DSSCs has not contributed to more than 12% of the highest recorded efficiency over the last 10 years [14,15]. Therefore, new sensitizers or semiconductors, which can replace organic dyes of ruthenium polypyridine complexes, are necessary to broaden the photoresponse in solar spectrum and increase the efficiency of DSSCs. Inorganic semiconductors, such as QD materials, can serve as dye replacements for next-generation sensitizers because of their exceptional optical properties [16–18]. QDs with tunable band gaps have opened an alternative path for harvesting light energy from visible to infrared (IR) regions of the solar spectrum [19–21].

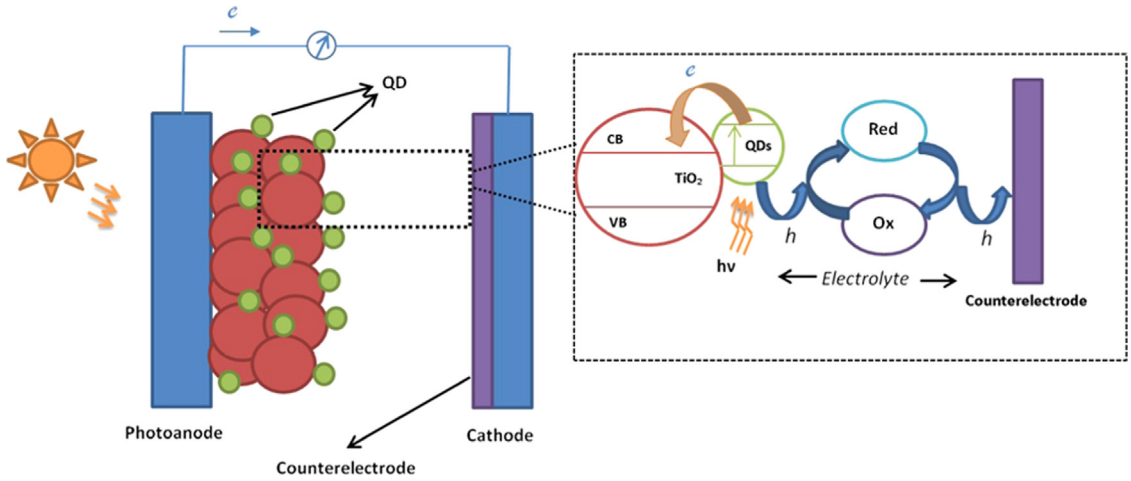

Fig. 2. Operating principle of a typical QDSSC.

QDs also possess competitive properties, such as multiple exciton generation, high molar extinction coefficients, sufficient photostability, and appropriate size dependency, resulting in the recognition of quantum dot-sensitized solar cells (QDSSCs) as a potential research subjects for future studies on solar cells. Multiple-exciton generation, which is known theoretically as the inverse Auger effect, contributes to the higher power conversion efficiency (η) of QDSSCs than that of DSSCs [22]. However, recent trends have shown that the overall conversion efficiency of QDSSCs is lower than that of DSSCs in terms of serious electron loss that results from charge recombination at the electrolyte–electrode or at the electrolyte–counter electrode interfaces [23,24]. The current study focuses on the use of different sensitizers to increase values of η by improving the light harvesting ability and the electron transfer rate of QDSSCs and by reducing the charge recombination rate at the interfaces [25,26].

To obtain this goal, a number of studies had explored different approaches, such as the use of multi-layered QDs on TiO_2, utilization of different-size of QD materials [27,28], and the use of different deposition methods, and of a passivation layer (e.g., ZnS) [29]. The passivation layer has been found to help exciton generation in the core to remove defects, such as unsaturated surface atoms on the surface, and to reduce alternative decay pathways. This paper highlights recent advances in the application of QDSSCs with different sensitizers that significantly affect the performance of QDSSCs in terms of incident photon-to-current efficiency (IPCE), short-circuit current density (J_{SC}), and open-circuit voltage (V_{OC}) values. At the end of this study, the advantages and disadvantages of QDSSCs with different QD sensitizer materials will be discussed. Recently encountered problems on the use of QDSSCs are also mentioned along with the proposed solution. Finally, this paper aims to promote future investigations on QDSSCs.

2. Basic principle of QDSSC

DSSCs consist of a dye-sensitized photoanode, a counter electrode, and an electrolyte (mostly iodide). The photoanode is composed of an oxide semiconductor material, particularly TiO_2, which is a highly stable solution under visible light illumination. Besides, a TiO_2 thin film can be prepared and sintered easily as the TiO_2 colloidal solution is coated on a transparent conductive oxide (TCO) substrate. The resultant film is normally 10 μm thick and exhibits a nanoporous structure that increases dye absorbance on the TiO_2 film [30]. The dye sensitizer (a Ru complex) is subsequently absorbed in the TiO_2 surface, which leads to photon absorption and electron injection. The electrolyte I^-/I_3^- is frequently used to transfer electrons between TiO_2 and the counter electrode. Tri-iodide ions, which are created by the reduction of dye cations with the I^- ion, are then reduced to I^- ions at the counter electrode. Pt- and carbon-based materials coated on the TCO substrate are generally used as counter electrodes. The physically blocked fluorine-doped tinoxide (FTO)–electrolyte interface effectively prevents the injected electrons in the FTO to recombine with the redox in the electrolyte [31].

The only difference between DSSCs and QDSSCs is the sensitizing material that is substituted by inorganic nanoparticle QDs in QDSSCs. Electron–hole pairs are created in the QDs as they progress from the lower to the excited state. Electrons from the conduction band (CB) of QDs are injected into that of TiO_2 (Fig. 2) upon illumination, resulting in the oxidation of the photosensitizer. The ground state of QDs is regenerated through electron donation from the electrolyte, which is commonly a redox system such as polysulfide $\left(S^{2-}/S_x^{2-}\right)$ redox couples. Another oxidation then occurs in the photoanode–electrolyte interface in the electrolyte [32–34].

$$S^{2-} + 2h^+ \rightarrow S \quad (1)$$

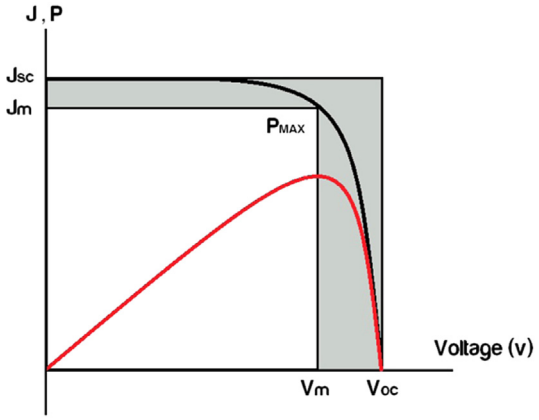

Fig. 3. Typical J–V and P–V curves of a QDSSC.

$$S + S_{x-1}^{2-} \rightarrow S_x^{2-} \quad (x = 2-5) \quad (2)$$

On the counter electrode, the oxidized groups S_x^{2-} are re-reduced to S^{2-}. Hence, electrons migrate via the external load to complete the circuit [33].

$$S_x^{2-} + 2e^- \rightarrow S_{x-1}^{2-} + S^{2-} \quad (3)$$

Subsequently, voltage is generated by variations in Fermi levels between the electron in the photoelectrode and the redox potential of I^-/I_3^- in the electrolyte. As a result, QDSSC devices generate electrical power through sunlight, and the η of the cells is obtained as follows [35,36]:

$$\eta = \frac{J_m V_m}{P} \quad (4)$$

where P is the power density at the operating point, and J_m and V_m represent current density and voltage, respectively, at the actual maximum power. Efficiency can also be estimated by using the fill factor (FF) [37].

$$\eta\,(\%) = \frac{J_{SC} \times V_{OC} \times \mathrm{FF}}{P} \times 100 \quad (5)$$

where J_{SC} and V_{OC} are short current density (mA/cm^2) and open circuit voltage, respectively. They are indicated by the direct current density–voltage (J–V) curves (Fig. 3). J_{SC} is dependent on light intensity, light absorption, injection efficiency, and regeneration of oxidized dye. V_{OC} is dependent on both the Fermi level of the semiconductor and the level of dark current. The maximum value of the open circuit voltage is determined by the difference between the Fermi level of the semiconductor and the redox potential of the hole conductor. The ideality of the cell is determined by FF, which is derived from the ratio of the inner ($J_m \times V_m$) to the outer ($J_{SC} \times V_{OC}$) rectangular area

$$\mathrm{FF} = \frac{J_m \times V_m}{J_{SC} \times V_{OC}} \quad (6)$$

Assuming that FF is equal to one, the J–V curve reaches the outer rectangular area. Several factors influence FF. One of these factors is high inner resistance (e.g., a bad counter electrode), which decreases FF and overall efficiency.

The probability of an incident photon transporting an electron to the outer circuit can be calculated by using short-circuit photocurrents (I_{SC}) at various excitation wavelengths (λ), The probability is calculated by

$$\mathrm{IPCE}\,(\%) = [1240 \times I_{SC}\,(A/\mathrm{cm}^2)]/[\lambda\,(\mathrm{nm})] \times I_{inc}\,(W/\mathrm{cm}^2)] \times 100\% \quad (7)$$

where I_{inc} is the incident light power, and J_{SC} is obtained by integrating the production of incident photon flux density $F(\lambda)$ and

IPCE(λ) in the range of wavelengths (λ) of the incident light. J_{SC} can be expressed as follows [35,19]:

$$J_{SC} = \int qf(\lambda)\mathrm{IPCE}(\lambda)d\lambda \tag{8}$$

where q is the electron charge. Alternatively, IPCE is given by the following equation:

$$\mathrm{IPCE}\ (\lambda) = \mathrm{LHE}(\lambda) \times \varphi_{inj} \times \eta_c \tag{9}$$

where φ_{inj} is the quantum yield of electron injection, η_c is the efficiency of collecting injected electrons at the back contact, and LHE is the light harvesting efficiency at a certain wavelength. LHE can be obtained as follows [30]:

$$\mathrm{LHE} = 1 - T = 1 - 10^{-Absorbance} \tag{10}$$

where absorbance refers to the light absorbed by the QDs. The number of injected electrons is equal to the number of electrons collected on the TCO, that is, any electron loss is due to charge recombination only. Therefore, η_c can be calculated as

$$\eta_c = J_{SC}/J_{inj} = J_{SC}/[J_{SC} + J_r] = 1 - [\tau_{SC}/\tau_{OC}] \tag{11}$$

where J_{SC} is the short circuit current density, J_{inj} is the electron injection current density from excited QDs to the anode, J_r is the recombination current density, τ_{SC} is the electron transit time, and τ_{OC} is the recombination time.

Internal quantum efficiency (IQE) is an important characteristic of a solar cell. It reveals how efficiently the absorbed photons are converted into current in the external circuit. For an ideal solar cell, IQE = 1. After accounting for loss due to light absorption ($\%T_{TCO}$) by the TCO substrate, the IQE of a solar cell at a certain wavelength can be calculated from the IPCE and LHE as follows [38]:

$$\mathrm{IQE} = \mathrm{IPCE}/[\%T_{TCO} \times \mathrm{LHE}] = \varphi_{inj} \times \eta_c \tag{12}$$

A standard measurement is needed to compare the efficiency of different research groups. For cell illumination, a standard solar spectrum of AM (air mass) 1.5 G (global) is used. This spectrum is derived from the path length the light needs to travel through the atmosphere and reach the surface. The spectrum is normalized so that the integrated irradiance is 1000 W/m^2 (100 mW/m^2) [38].

3. QD material in QDSSCs

Unlike bulk semiconductor, semiconductor QDs are spherical nanomaterials with special optical properties and are less than 10 nm in size [39]. QDs have many advantages, such as (i) hot carrier injection from higher excited state to the CB of TiO_2 through light irradiation [40], (ii) multiple exciton generation (MEG) of carrier [41], and (iii) tunable band gap and size-dependent properties as a result of quantum confinement that enhances the charge separation and absorption of solar cells [42].

Various QD materials have been investigated in QDSSCs because of their particular properties for photosensitization. These materials include CdS, CdSe, PbS, ZnSe, CdHgTe, CdTe, InP, and Ag_2S. Among these QD materials, CdSe and CdS are frequently used because of their ease of fabrication and characterization [43].

3.1. Multiple exciton generation

Given the nature of photovoltaic materials, light absorbing materials will absorb only certain amounts of energy from incident photons. A major problem in traditional solar cells, which restricts cell conversion efficiency, is that the incident photon with the excess energy above the semiconductor band gap is lost through heat because of electron–phonon scattering and subsequent carrier replacement to the lower state by phonon emission [44]. The main approach to reduce this loss is MEG, in which the number of excitons produced by a single photon is restricted by energy conversion. In other words, photons with E_g, $2E_g$, and $3E_g$ energies produce one, two, and three excitons, respectively (Fig. 4). Another technique that can be used to enhance conversion efficiency is

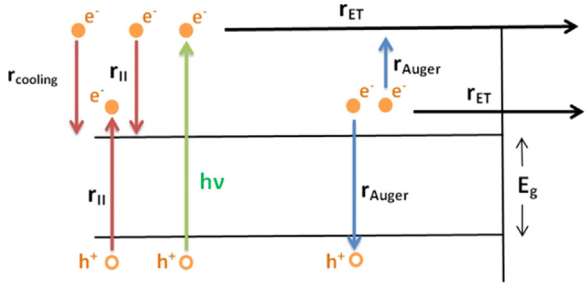

Fig. 5. Dynamical channels for photo-induced hot electron–hole pair [29].

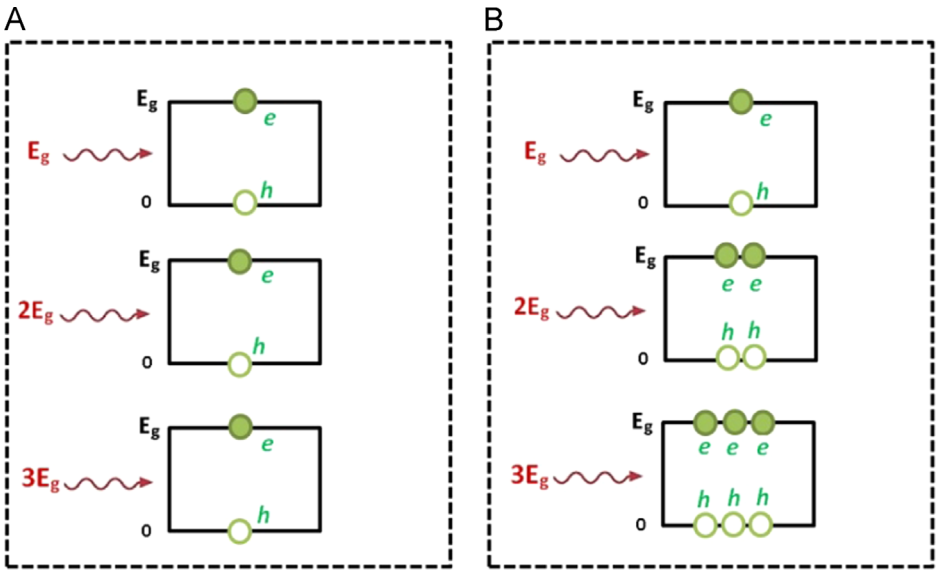

Fig. 4. (A) Traditional schematic of solar cell and (B) multiple excitons are generated through single phonon.

through the utilization of carriers before they are transferred to the lower band edge as a consequence of phonon emission. This effect was first demonstrated in CdSe QDs by Guyot-Sionnest et al. [44].

Two fundamental methods can be used to utilize hot carriers. One is to produce and to enhance the photocurrent, and another is to produce an enhanced photovoltage. The former requires hot carriers to generate more electron–hole pairs, while the latter involves the extraction of hot carriers from the photo-converter before they cool [45]. The extraction process is called impact ionization (I.I.) and is the opposite of the Auger process, in which two electron–hole pairs are recombined to produce a powerful electron–hole pair. To enhance the photocurrent, the rate of I.I. ($r_{I.I.}$) or e–h pair multiplication should be higher than the rates of electron transfer (r_{ET}), carrier cooling ($r_{cooling}$), and of the Auger processes (r_{Auger}). The schematic of the energies is illustrated in Fig. 5 [46]. Highly efficient MEG has been studied by Ellingson et al. [47] using PbS and PbSe QDs. Meanwhile, Schaller et al. [48] showed that the carrier multiplication (CM) factor is negligible in InAs QDs. This finding was in contrast to the results obtained by Ben-Lulu et al. [49] in 2008, provided strong evidence on the occurrence of MEG in InAs/CdSe/ZnSe QDSSCs.

3.2. Charge transfer process

After excitation, charge separation occurs at the interface between the band gap of the semiconductor/QD and the electrolyte in QDSSCs, followed by electron–hole pair generation [25,50].

$$QD + h\nu \rightarrow QD(e_p + h_p) \rightarrow QD(e_s + h_s) \quad (13)$$

$$QD(e_s + h_s) \rightarrow QD + h\nu \quad (14)$$

The notations s and p represent the lower and the higher electronic states of the electron and the hole, respectively. The charge transfer then occurs as follows:

$$QD(e_s) + TiO_2 \rightarrow QD(h_p) + TiO_2(e) \quad (15)$$

$$QD(h_p) + \text{Red} \rightarrow QD + O_X \quad (16)$$

where O_x and Red are the oxidation and reduction of the electrolyte, respectively. Charge separation in QDs is enhanced by an alternative deactivation pathway created as a result of decreasing particle size.

When the electron–TiO_2 pathway is the only additional deactivation pathway for the excited state between TiO_2 and QDs, the rate constant is calculated by comparing the bleaching lifetimes in the presence and absence of TiO_2. For example, the k_{et} of CdSe QDs with diameters of 2.6 and 3.7 nm on sphere-like TiO_2 films is e-fold by 2.5×10^9 and 0.63×10^9 s^{-1}, respectively [25].

$$k_{et} = 1/\tau_{QD+TiO_2} - 1/\tau_{QD} \quad (17)$$

In general, electrolyte solutions with different pH values when in contact with the photoanode can also moderate charge injection process, as observed in the fluorescence spectra reported by Chakrapani et al. [51]. Meanwhile, the TiO_2 CB will shift to a more negative potential by assuming a high-pH electrolyte. Consequently, the energy difference between QD and TiO_2 CBs will decrease along with the electron injection rate.

Moreover, the electron injection rate can be changed by employing different numbers of successive ionic layer adsorption and reaction (SILAR) deposition cycles. Shen et al. [52] demonstrated that the rate of electron injection times increases from 2.8 ps to 6.3 ps as the number of SILAR deposition cycles increases from 2 to 15. Consequently, results of their study showed that electron relaxation time increased from 83 ps to 320 ps subsequently. Thus, the rate of electron injection from QDs to TiO_2 can be reduced considerably by increasing the frequency of deposition cycles.

Table 1
QDSSCs with different QD diameter.

QDs	Diameter (nm)	J_{SC}	V_{OC}	λ Region	IPCE (%)	Ref.
CdS	4.4	3.519	0.41	350–470	0.66	[23]
CdS	4.9	4.519	0.44	350–500	0.85	[23]
CdS	5.9	6.694	0.48	350–525	1.29	[23]
CdS	6.2	5.494	0.51	350–550	1.05	[23]
$CuInS_2$	8.27	4.22	0.355	400–800	0.46	[20]
CdSe/N719	2.2	2.37	0.75	400–700	0.71	[28]
CdSe/N719	2.5	6.42	0.78	400–650	3.31	[28]
CdSe/N719	3.3	6.95	0.81	400–600	3.65	[27]
CdSe(I)	2.5	2.25	0.59	400–550	0.53	[27]
CdSe(II)	3.5	3.23	0.64	400–600	0.86	[27]
CdSe(I)/CdSe II	2.5/3.5	3.41	0.66	40–650	1.26	[27]

Moreover, the increase in the charge recombination rate between the photoanode and the electrolyte resulted from a slow electron transfer rate. One method of preventing this recombination is by coating QDs with a protective layer that has a higher band gap than that of QDs Such as ZnS layer which is commonly used for CdS and CdSe QDs. The ZnS coating material contributes to passivation of the surface of QDs by suppressing the surface trapping of photo-excited electrons and holes in QDs. The J_{SC} and IPCE values eventually increase as a result of the transfer of efficient photo-excited electrons into TiO_2 CB. This phenomenon is consistent with the results obtained by Li [53] and Tubtimtae [54] for CdS and for Ag_2Se QDs, respectively.

3.3. Size-dependent band gaps

The major advantage of using QDs as sensitizers in QDSSCs is the size-dependent band gap, which is a characteristic of the optical properties of QDs. By varying the size of QDs, the light harvesting energy in the solar spectrum can be controlled [18]. Moreover, an efficient charge separation can be optimized by tuning the QD size based on the quantization effect.

Size dependency is due to the quantum confinement effect exhibited by QD [55]. The quantum confinement effect is manifested when the QD solution exhibits a different color that corresponds to the change in the particle size. This change in size affects a different light absorption band. When QD particles are sufficiently small in size, the effective band gap energy of QDs becomes wider. Subsequently, optical absorptions and emissions in relation to excitations across the band gap shift toward higher energies [36]. Quantum size effects were previously examined by Gorer et al. [56] who observed the blue shift of the optical spectra of CdSe films as crystal size decreased. Although photon absorption by bigger particles in the visible region is more significant than that by smaller particles, electrons cannot be effectively inserted into TiO_2 unlike with smaller-sized QDs [25].

Recently investigated QDSSCs with different QD diameters at different wavelength regions are summarized in Table 1. In the corresponding wavelength region, each QDSSC has unique IPCE characteristics. For example, the photocurrent increases as the particle size of CdS increases because of the improvement in QDs on the TiO_2 surface. This phenomenon reduces the recombination between TiO_2 and the electrolyte, which is followed by an increase in the charge collection efficiency. As a result, higher IPCE is obtained for CdS with a diameter of 5.9 nm [23].

In another way, CdSe/N719 QDs with different sizes (2.2, 2.5, and 3.3 nm) yield different IPCE values and perform at different wavelength regions (from 380 nm to 700 nm, 380 nm to 650 nm, and 380 nm to 600 nm, respectively). Moreover, J_{SC} increases with particle size, whereas V_{OC} remains nearly constant. These

results imply that the low current density and V_{OC} of the reported CdSe QD (2.5 nm) are due to the low loading of CdSe QDs on TiO_2. In addition, the small pore size of the TiO_2 electrode can restrict the formation of a compact monolayer on the CdSe QD sensitizer [28].

$CuInS_2$ has also been shown to absorb light in a wavelength range of 400–800 nm. In addition, this material can theoretically provide higher values of J_{SC} than those of CdS, however, the IPCE values provided by $CuInS_2$ are significantly lower than those provided by CdS because of low coverage on the TiO_2 surface [20,34].

Meanwhile, the use of two different sizes of QDs has resulted in improved performance compared with that of single-sized cells. Lei et al. [27] showed that CdSe QDSCs exhibit an efficiency of 1.26%, which is higher than that of single-sized cells (1%). The electron lifetime of the device based on TiO_2/CdSe QD (2.5 nm)/CdSe QD (3.5 nm) is longer than that of devices based on TiO_2/CdSe QD (2.5 nm), which indicates that the charge recombination at the interface is lessened by sensitizing two types of CdSe QDs [27]. Therefore, combining different sizes of QDs with other sensitizers in a cell achieves better efficiency than combining only one size of QDs because of the wider light absorption by QDs with a wide range of band gaps.

4. QDs as sensitizers in QDSSCs

QD sensitizers can be synthesized by two fundamentally different techniques [57]: in situ fabrication and attachment of pre-synthesized colloidal QDS (ex situ fabrication). Not only these techniques are simple, but also they are applicable in large-scale production. However, they do not provide precise control of the particle size distribution of the QDs. The former (in situ technique) is commonly used for QD preparation and includes chemical bath deposition (CBD) and SILAR. It performs better than the latter (ex situ technique) when used to assemble QDSSC [58].

CBD is a relatively simple method of depositing QDs and nanoparticle films when the growth of QDs occurs in one bath. Cationic and anionic solutions are prepared separately and placed in a container to form a bath solution for slow reaction. QDs are grown on the surface of the wide-band gap semiconductor by dipping the electrode into the bath solution for a defined period. Thus, QD deposition is controlled by varying the dipping time. This method also possesses many advantages, such as stable yield, robust adherence, and uniform and good reproducibility. However, the growth of QDs strongly depends on growth conditions, such as deposition duration, solution composition and temperature, and mesoporous film characteristics [59].

In SILAR, cationic and anionic precursors are separately placed in two beakers or containers. TiO_2-coated electrode is dipped into the cationic precursor solution and then into the anodic precursor. Each dipping step is followed by rinsing and drying. The two-step dipping procedure is regarded as one deposition or SILAR cycle. The size of the deposited QDs can be controlled by the number of dip cycles [60]. Senthamilselvi et al. [61] reported that SILAR is a better approach than CBD because of its shorter processing time and close stoichiometry formation.

Aside from CBD and SILAR, QDs can also be prepared through ex situ fabrication by using molecular linkers that have various functional groups. In this technique, QDs are pre-synthesized by using capping agents, such as mercaptopropionic acid, trioctylphosphine, and trioctyphosphine oxide. QDs can also be deposited directly without using linker molecules via direct absorption, which may lead to a high degree of QD aggregation in addition to low surface coverage. This technique also enables precise control over the size and hence the spectral absorption properties of the QDs [62,63]. However, these techniques only develop the performance of QDs as sensitizers in the fabrication of QDSSCS. Optimization studies should be conducted to increase the energy conversion efficiency of QDs.

To this end, an approach that utilizes different types of sensitizers in QDSSCs must be developed for a better and simpler comparison. In this review, the maximum values of significant factors, namely, FF, V_{OC}, η, and J_{SC}, are considered with respect to the QD material for each QDSSC. The highest J_{SC}, V_{OC}, FF, or η values of different sensitizers are then compared (Table 1). The types of semiconductor material, counter electrode, and electrolyte are also considered for a better comparison.

The QDs employed in QDSSCs as sensitizers include $CuInS_2$ [20], PbS [64,65], $AgInSe_2$ [66], PbSeS [67], Ag_2Se [54], CdS [68], CdSe [69], CdTe [70], and ZnS [29]. Among these sensitizers, CdS and CdSe QDs have been considered as adequate choices as stable materials in QDSSCs [43]. Improvements observed on the performance of the cells incorporated with the sensitizers are mainly attributed to the increase in QD size and in the surface area covered by the QDs on the photoelectrode.

Another method to improve QDSSCs was reported by Yu et al. [71]. In this method, CdSe/CdS core/shell nanocrystals were used. The CdSe/CdS core/shell structure exhibited higher J_{SC}, V_{OC}, and η than those of single CdSe QD-sensitized solar cells. Besides, CdSe/CdS QD prevented charge recombination inside QDs by reducing the surface states and by accelerating charge separation. Hence, single QDs is incapable of increasing energy conversion efficiency of QDSSCs to high levels.

Jung et al. [23] developed another approach to improve QDSSC performance. The method involves a passivation layer (e.g., ZnS) between TiO_2 and the electrolyte in CdS QDs. The passivation layer reduced the recombination rate from TiO_2 to the electrolyte, resulting in increased charge collection efficiency. This result was also demonstrated in PbS QDSSCs with a CdS coating layer [65].

Multi-layered QDs fabricated using the chemical bath deposition (CBD) method can likewise improve QDSSC performance. The highest QDSSC efficiency achieved by Hu et al. was 1.47% for CdS/$CuInS_2$. However, with a single QD, efficiency rates of only 0.34% and 0.38% were reported for CdS and $CuInS_2$ QDSSCs, respectively. Therefore, CdS inhibits interfacial recombination, consequently increasing V_{OC} and efficiency [72]. Meanwhile, dye sensitizers used in DSSCs can improve solar cell performance when coupled with QD sensitizers. Fan et al. [73] reported that co-sensitized solar cells with QDs significantly improve photocurrent and power conversion efficiency rates (7.265 mA/cm^2 and 1.03%, respectively) compared with those of QDs alone or of DSSCs (0.09% and 0.41%, respectively).

Different annealing temperatures (100 °C, 150 °C, 200 °C, and 250 °C) also affect QDSSC performance, as reported by Yu et al. [71]. Annealing treatment of CdSe/CdS QDs increased IPCE from 0.46% to 2.83%. A remarkable efficiency of 4.21% was obtained when a TiO_2/CdSe/CdS/ZnS photoanode was annealed at 300 °C. The cell prepared with the same photoanode but without heat treatment yielded an efficiency of only 3.20%.

Other factors, such as counter electrode and electrolyte materials, must also be considered to improve QDSSC performance. CuS and CoS are two counter electrodes used in ZnS/CdSe/CdS multilayer QDSSCs. The use of these counter electrodes yielded efficiencies of 2.7% and 1.9% respectively. These results indicate significant enhancement in IPCE compared with that of a Pt counter electrode with an efficiency of 1.6% [29].

The use of different electrolyte materials may also lead to increased QDSSC performance. Karageorgopoulos et al. [74] employed two different electrolytes, namely, a quasi-solid electrolyte that contains polysulfide (S^{-2}/S_x^{-2}) and a hybrid organic–inorganic ICS-PPG230 material in ZnO/CdS/CdSe QDSSCs. The fabricated solar cell enhanced the solar cell conversion efficiency from 1.2% to 4.5%. The results showed that the quasisolid

Table 2
QDSSCs using different sensitizers.

Number	Oxide semiconductor	Sensitizer	Counter electrode	Electrolyte	V_{OC} (V)	J_{SC} (mA/m^2)	FF (%)	η (%)	Ref.
1	TiO_2	CdS/ZnS	Pt	0.5 M Na_2S, 2 M S, 0.2 M KCl in water/methanol solution	0.51	7.813	46.5	1.72	[23]
2	TiO_2	CdS	Pt	0.5 M Na_2S, 2 M S, 0.2 M KCl in water/methanol solution	0.51	6.69	45.9	1.29	[23]
3	ZnO/Zn_2SnO_4	CdS	Pt	0.5 M Na_2S, 2 M S, 0.2 M KCl in water/methanol solution	0.71	3.10	41.8	0.92	[76]
4	ZnO	CdS	Pt	0.5 M Na_2S, 2 M S, 0.2 M KCl in water/methanol solution	0.68	1.30	30	0.25	[24]
5	TiO_2	CdS/$TiCl_4$ treatment	Pt	0.5 M Na_2S, 1 M S, 0.2 M KCl in water/methanol solution	0.49	4.05	32.8	0.65	[24]
6	TiO_2	Si QD	Pt	0.5 M Na_2S, 2 M S, 0.2 M KCl in water/methanol solution	0.11	0.64	–	0.02	[77]
7	N-TiO_2	$CdSe_xS_{1-x}$/CdSe	Pt	2 M Na_2S, 0.5 M S, 0.2 M KCl in water/methanol solution	0.48	12.03	65	3.67	[78]
8	TiO_2	CdS/CO/ZnS	Pt	0.5 M Na_2S, 2 M S, 0.2 M KCl in water/methanol solution	0.50	6.541	43.4	1.33	[79]
9	TiO_2	Sb_2S_3	Pt	Polyanilin hole conductor	1.09	1.76	53.1	3.78	[80]
10	TiO_2	$CuInS_2$	Pt	0.24 M Na_2S, and 0.035 M Na_2SO_3 in aqueous solution	0.37	4.22	32	0.46	[20]
11	TiO_2	$CuInS_2/In_2S_3$	Pt	0.24 M Na_2S, and 0.035 M Na_2SO_3 in aqueous solution	0.56	4.51	41	1.06	[20]
12	TiO_2	Si QD	Pt	Polysulfide $\left(S^{-2}\,S_2^{-2}\right)$	–	–	–	0.02	[81]
13	TiO_2	Nitridated Si QD	Pt	Polysulfide $\left(S^{-2}\,S_2^{-2}\right)$	–	–	–	0.04	[81]
14	TiO_2	CdHgTe/CdTe	Pt	1 M LiI, 1 M I_2	0.76	4.43	62	2.2	[70]
15	TiO_2	CdHgTe	Pt	1 M LiI, 1 M I_2	0.66	3.41	54.6	1.0	[70]
16	TiO_2	CdS	Pt	2 M Na_2S, 2 M S	0.35	2.57	18	0.17	[68]
17	TiO_2	CdS	Carbon electrode	2 M Na_2S, 2 M S in aqueous solution	0.45	5.57	58	1.47	[68]
18	TiO_2	CdSe	Cu_2S	Polysulfide	0.57	13.9	53	3.83	[69]
19	TiO_2	ZnSe/CdS Type II	Pt	Na_2S (0.5 M), S (0.125 M), KCL(0.2 M) in water/methanol	0.44	2.29	27	0.27	[82]
20	ZnO nanorod	CdSe	Pt	0.1 M I_2, 0.1 M LiI, 0.5 M tert butylpyridine, 0.6 M iodide in methoxyacetonitrile	0.58	2.70	47.4	0.74	[83]
21	Graphene–TiO_2 film	CdS	Pt	0.5 M Na_2S, 2 M S, and 0.2 M KCl in water/methanol	0.57	7.19	41	1.31	[84]
22	Graphene	CdS	Pt	1 M KNO_3	–	–	–	1.2	[85]
23	Graphene–TiO_2	CdS	Au	0.5 M Na_2S, 2 M S, and 0.2 M KCl in water/methanol	0.58	7.1	43	1.44	[21]
24	TiO_2	$AgInSe_2$	Pt+Hg/Hg_2SO_4	Cobalt ion dissolve in acetonitrile and ethylene carbonate	0.63	0.92	45	0.26	[66]
25	SWCNT/TiO_2	PbS	Pt	LiI (0.1), I_2 (0.05) in acetonitrile	0.48	3.02	44	0.80	[86]
26	TiO_2	PbS	Pt	LiI (0.1), I_2 (0.05) in acetonitrile	0.44	2.62	41	0.59	[86]
27	ZnO/VACNTs	CdSe	Pt	2 M Na_2S, 3 M S	0.57	4.45	57.5	1.46	[87]
28	ZnO	CdSe	Pt	2 M Na_2S, 3 M S	0.54	3.86	42.7	0.88	[68]
29	ZnO	ZnPc+PbS	Au	KI (0.5 M), I_2 (0.05)	0.30	1.42	34.8	0.69	[88]
30	ZTO	ZnPc+PbS QD	Au	KI (0.5 M), I_2 (0.05)	0.32	1.38	40.9	0.85	[89]
31	TiO_2/ZnO CdS		Au	0.5 M Na_2S, 2 M S, and 0.2 M KCl	0.58	7.66	35	1.56	[90]
32	TiO_2	CdS	Au	0.5 M Na_2S, 2 M S, and 0.2 M KCl	0.49	5.52	36	0.99	[91]
33	TiO_2	ZnS/CdSe/CdS	CoS	1 M Na_2S, 1 M S,	–	11.2	32	1.9	[57]
34	TiO_2	ZnS/CdSe/CdS	CuS	1 M Na_2S, 1 M S,		13.9	35	2.7	[57]
35	TiO_2	ZnS/CdSe/CdS	Pt	1 M Na_2S, 1 M S,	–	9.1	35	1.6	[57]
36	TiO_2	CdS/PbS	Pt	Polysulfide	11.5	0.581	30	2.02	[65]
37	TiO_2	PbS/CdS	Pt	Polysulfide	0.34	1.21	35	0.15	[65]
38	TiO_2/ZnS	CdSe/CdS	Cu_2S	1 M Na_2S, 1 M sulfur in water	0.65	13.56	66	4.21	[68]
39	ZnO	CdS	Zinc	0.1 M $Zn(NO_3)_2$ 0.1 M KCl	0.53	7.9	30	1.16	[90]
40	TiO_2	$CuInS_2$	Carbon	1 M Na_2S, 1 M S	0.23	4.44	37	0.38	[72]
41	TiO_2	CdS/$CuInS_2$	Carbon	1 M Na_2S, 1 M S	0.48	8.12	37	1.47	[72]
42	TiO_2	CdS	Carbon	1 M Na_2S, 1 M S	0.31	2.48	45	0.34	[72]
43	TiO_2/ZnS	Ag_2Se	Pt	0.5 M Na_2S, 2 M S, and 0.2 M KCl, 0.5 M NaOH	0.15	33.3	24.3	1.21	[54]
44	TiO_2/ZnS	Ag_2Se	Pt	Iodide/triiodide	0.27	28.5	23.8	1.76	[54]
45	TiO_2	PbS	Cu_2S	1 M Na_2S, 1 M S, and 0.1 M NaOH in water	0.42	7.3	61	1.9	[67]
46	TiO_2	PbSeS	Cu_2S	1 M Na_2S, 1 M S, and 0.1 M NaOH in water	0.41	6.4	63	1.58	[67]
47	TiO_2	PbS/CdS	Cu_2S	1 M Na_2S, 1 M S, and 0.1 M NaOH in water	0.46	8	58	2.1	[67]
48	Zn_2SnO_4	CdS	Pt	0.6 M 1,2 dimethyl.3.n.propylimidazolium iodide, 0.1 M LiI, 0.05 M I_2 in acetonitrile	0.48	0.49	45.5	0.10	[70]
49	Zn_2SnO_4 treated Al^{3+}	CdS	Pt	0.6 M 1,2 dimethyl.3.n.propylimidazolium iodide, 0.1 M LiI, 0.05 M I_2 in acetonitrile	0.49	0.86	61	0.26	[70]
50	TiO_2	CdSe	Pt	0.5 M Na_2S, 2 M S in methanol/H_2O	0.40	3.181	45.6	0.59	[73]
51	TiO_2	CdSe+dye (JK24)	Pt	0.5 M Na_2S, 2 M S in methanol/H_2O	0.45	6.705	38.2	1.18	[73]
52	Zn_2SnO_4/ZnS	CdS	Pt	0.6 M 1,2 dimethyl.3.n.propylimidazolium iodide, 0.1 M-LiI, 0.05 M-I_2 in acetonitrile	0.43	0.27	47.4	0.05	[53]
53	TiO_2 nanocoral	PbS	Pt	0.5 M-NaOH, 0.5 M-polysulfide, 0.5 Na_2S	0.32	3.84	49	1.23	[64]
54	ZnO	CdS/CdSe	Pt	Polysulfide $\left(S^{-2}/S_x^{-2}\right)$ redox (aqueous)	0.53	7.6	30	1.2	[74]
55	ZnO	CdS/CdSe	Pt	ICS-PPG230 (Quasi solid)	0.68	16.3	41	4.5	[74]

electrolyte was more appropriate than the aqueous electrolyte because the former reduced the leakage as well as the sealing problem in the cells.

As shown in Table 2, CdS/CdSe with a ZnO semiconductor incorporated with the quasi-solid electrolyte displays the highest efficiency and J_{SC} (4.5% and 16.3 mA/cm^2, respectively) [74]. These findings indicate that among QD sensitizers, CdS and CdSe QDs, particularly in the form of multi-layered QDs incorporated with a passivation layer (CdS/CdSe/ZnS), exhibited the highest performance. These QDs can be further improved by replacing the Pt counter electrode with other electrolytes, such as Cu_2S or CuS [71].

5. Advantages of QDs

Recent developments in technology have replaced the costly, inefficient, bulk material for QDs, significantly contributing to the increased range of QD applications [42]. The size of the produced dot can be fully controlled by providing accurate supervision over the wavelength of the emitted photon. It states that, the color of the emitted light from QDs can be highly tuned at a negligible cost and with affordable technology. A complete range of QDs, each characterized by a distinct and narrow emission spectrum, can therefore be produced [90]. Moreover, the low energy requirement for excitation can be provided by a single visible light or ultraviolet wavelength beam regardless of QD size. These properties significantly reduce production costs [39–41].

QDs can also be used in a wide range of experiments, particularly in highly sensitive applications, such as QDSSCs, because of their high photostability regardless of time limitations. The range of applications can be further expanded by utilizing alternative forms of QDs, such as quantum dust, beads, and crystalline forms [30].

Finally, QDs can be provided by various economical and simple development methods, such as colloidal synthesis and lithographic and epitaxial techniques [91].

6. Limitations and challenges

Although many high-quality QDs have been used as alternative sensitizers in QDSSCs, many of them do not produce highly efficient QDSSCs. Several difficulties limit the overall efficiency of the cell and require consideration in future investigations.

Likewise, the specific energy band gap of single QD-sensitized solar cells is a major problem because it restricts the absorption of sensitized QDSSC films to the specific region, particularly for CdS QDSSCs which is in visible region [65]. Meanwhile, the incorporation of a dye material in QDs to widen the absorption spectrum may overlap absorption areas at short wavelengths of both sensitizers, which results in sharing of incident photons at this wavelength region. This phenomenon decreases the IPCE value as a result of the low photo-to-current conversion efficiency of QDs [73].

The major problem in QDSSCs is recombination loss. Electrons that are photo-injected into TiO_2 recombine with the redox couple in the electrolyte. In some cases, such as that in $CuInS_2$ QDs, this recombination occurs as a result of band misalignments and of high surface-state density in the heterostructure between TiO_2 and QDs [20]. Similarly, the large particle size of Si QDSSCs increases the recombination loss with the redox electrolyte in the Si–TiO_2 network [77].

Moreover, low QD loading and the subsequent weak electronic connection between QDs and TiO_2 introduce defects in cell performance and subsequently reduce cell efficiency. This problem can be addressed by introducing excess QDs onto the TiO_2 surface by SILAR, CBD, or other methods that can increase QD loading. However, Zhao et al. [84] and Chen et al. [92] stated that excess QDs can act as recombination centers in the presence of CdS or graphene QDs by increasing the surface area exposed to the electrolyte, which leads to high electron recombination loss.

Furthermore, different electrolytes have different effects on QDSSC efficiency, further restricting the overall efficiency of the cell. Solar cells provided by PbS and PbSeS QDs with polysulfide electrolyte exhibit low stability as PbS corrodes in the polysulfide electrolyte. Therefore, direct contact between PbS and the electrolyte must be avoided [67]. Similarly, 73% reduction in the overall efficiency of the cell was observed in ZnO/CdS/CdSe/ZnS multilayer QDs when the quasi-solid electrolyte was replaced with an aqueous electrolyte [74].

Considering the limitations and challenges associated with QDSSCs, researchers have more room to explore and understand the use of new materials in improving the performance of QDSSCs.

7. Conclusions

This feature article provides a review of nanomaterials that have been used as sensitizers in the fabrication of QDSSCs. With advances in nanotechnology, QDSSC performance has been significantly improved (Table 2). QDSSCs that provide η values of more than 4% have been prepared [65,74]. These high η values can be attributed to increased electron transport, light harvesting, and decreased inner energy loss.

To enhance the light-harvesting energy transfer, QDs can be used in conjunction with organic dyes or with other QDs (multilayered QDs). However, a distinct electrode on which CdSe QDs and organic dye molecules are spatially organized must be developed to increase IPCE to a higher value [54]. In a similar manner, the co-presence of CdSe in CdS QDs with an energy band gap of 2.25 eV can effectively extend the absorption region [74].

Furthermore, surface modification can also be used to minimize the recombination loss. A TiO_2 layer which is grown from $TiCl_4$ on a TiO_2-nanoparticle electrode is widely used to improve the conversion efficiency in QDSSCs [24]. In addition, coating QDs with a protective ZnS layer has been shown to prevent electron leakage into the electrolyte, thereby reducing the recombination loss [23].

Simultaneous use of several types of QD materials (e.g., $CuInS_2$/CdS QDSSCs) is recommended to widen the light absorption wavelength range of QDSSCs and to overcome limitations, such as $CuInS_2$/CdS QDSSCs particularly for cells with low electric conversion efficiency rates [72].

For cases in which the QD loading onto the TiO_2 surface is low, SILAR or CBD is an effective method of loading QDs on the TiO_2 layer. However, high performance is not always achieved in highly efficient SILAR or CBD cycle. For example, the highest performance for $ZnSnO_4$–CdS QDs was obtained at a maximum of six cycles [75]. In general, QDs produced by CBD exhibit higher cell performances than those produced by SILAR. The advantage of the SILAR method is that it can cover a large surface area of ordered TiO_2 nanostructures. In addition, the limitations in the photoanodes prepared by SILAR can be mitigated by effective passivation of the photoanode surface.

Another challenge associated with QDSSCS is substrate restriction. For instance, in CdS quantum-dot-sensitized Zn_2SnO_4 solar cells, the impedance of the ITO glass increases after calcination, subsequently improving charge recombination [53].

By considering the abovementioned difficulties and then forward proposed solutions of recent QDSSCs, researchers can have more flexibility in exploring and developing alternative methods and materials to improve the performance of QDSSCs.

In conclusion, 4.92% is the maximum reported energy conversion efficiency of QDSSCs with CdS/CdSe as sensitizer in the presence of polysulfide electrolyte [93]. Therefore, multi-junction PbS and CdS QD-based solar cells have the potential to enhance the power conversion efficiency by up to 10%. A recent study reported PbSe-based solar cells that exhibit over 100% external quantum efficiency [94], which is significant for their low fabrication cost and ability to efficiently harvest the sun light to near-infrared offers great promise for the design of QD-based solar cells with efficiency rates beyond the Shockley–Queisser limit. Recent studies have also shown that PbS QD solar cells can be stable for over 1000 h under continuous illumination [95]. Therefore, It can

be conclude that, lead chalcogenide PV can provide the three necessary economic major issues: cost, efficiency, and stability. Comparatively, Wadia et al. [96] reported that PbS materials for solar cells are naturally abundant in terms of raw material cost.

In terms of global energy market price, the price of QDSSC is expected to be less than that of the current DSSC ($3/Wp–$4/Wp) [11,12] because of the low-cost materials used, such as carbon-based counter electrode or carbon QDs. On the basis of the current market price of solar cells, this technology costs much lower than silicon solar cells ($3/Wp) [12].

Consequently, QD semiconductors have a high potential benefits to become new-generation energy devices because of their distinct optical and electrical properties, great surface area, high chemical stability, and high photostability. Recent studies have applied chemical engineering at the nanocrystal surface to better passivated the nanocrystal and reduce detrimental trap states which would reduce device performance by means of carrier recombination. The latest results in an efficiency of 7% which is among the highest achieved for QDSSCs and, although lower than commercial bulk silicon cells (17%), it has a potential for improvement beyond silicon cells due to hot carrier extraction and efficient multiple exciton generation [97]. With the advances in nanotechnology, some problems commonly encountered in QDSSCs may be partially solved and we expect major breakthroughs in developing QDSSCs in the near future.

For further development, future studies should focus on improving the performance of solar cells by (1) designing new semiconductor QDs with a large wavelength range of optical absorption, (2) improving the electronic interaction between QDs and electron acceptors, (3) improving QD loading onto the TiO_2 to increase the light harvesting efficiency of QDs, (4) minimizing the recombination loss at the interface of photoanode and electrolyte, (5) increasing electron mobility and device stability, and (6) reducing fabrication costs. Indeed, commercialization of large-scale solar cells based on nanostructure architecture has yet to be realized. QDSSCs have a potential to replace a dye for dye-sensitized solar cell and reduce material for any thin film or tandem solar cells as well as to compete with silicon solar cell in future.

Acknowledgments

The authors acknowledge the financial assistance provided by Universiti Teknologi Malaysia, the Malaysia–Japan International Institute of Technology (MJIIT) and the Exploratory Research Grants Scheme (ERGS) (1/2012/TK07/UKM/03/5) of the Malaysian Ministry of Higher Education. The authors also acknowledge and appreciate the contribution of the Solar Energy Research Institute (SERI) of Universiti Kebangsaan Malaysia.

References

[1] Holdren JP. Science and technology for sustainable well-being. Science 2008;456:424–34.
[2] Lior N. Energy resources and use: the present situation and possible paths to the future. Energy 2008;33:842–57.
[3] Kamat PV. Meeting the clean energy demand: nanostructure architectures for solar energy conversion. J Phys Chem C 2007;111:2834–60.
[4] Barnham KWJ, Mazzer M, Clive B. Resolving the energy crisis: nuclear or photovoltaics. Nat Mater 2006;5:161–4.
[5] Meyer GJ. Molecular approaches to solar energy conversion with coordination compounds anchored to semiconductor surfaces. Inorg Chem 2005;44:6852–64.
[6] Gratzel M. Photoelectrochemical cell. Nature 2001;414:338.
[7] Saga T. Advances in crystalline silicon solar cell technology for industrial mass production. NPG Asia Mater 2010;2:96–102.
[8] Ooyama Y, Harima Y. Molecular designs and syntheses of organic dyes for dye-sensitized solar cells. Eur J Org Chem 2009;18:2903–34.
[9] Shockley W, Queisser HJ. Detailed balance limit of efficiency of p–n junction solar cells. J Appl Phys 1961;32:510–9.
[10] Conibeer G. Third generation photovoltaic. Mater Today 2007;10:42–50.
[11] Kroon JM, Bakker NJ, Smit HJP, Liska P, Thampi KR, Wang P, et al. Nanocrystalline dye-sensitized solar cells having maximum performance. Prog Photovolt 2007;15:1–18.
[12] Kalowekamo J, Baker E. Estimating the manufacturing cost of purely organic solar cells. Sol Energy 2009;2009(83):1224–31.
[13] O'Regan, Gratzel M. Low-cost A. High-efficiency solar cell based on dye-sensitized colloidal TiO_2 films. Nature 1991;353:737–40.
[14] Yella A, Lee H-W, Tsao HN, Yi C, Chandiran AK, Nazeeruddin MK, et al. Porphyrin-sensitized solar cells with cobalt (II/III)-based redox electrolyte exceed 12 percent efficiency. Science 2011;334:629–33.
[15] Gratzel M. Dye-sensitized solar cells. J Photochem Photobiol C: Photochem 2003;4:145–53.
[16] Choi Hongsik, Nahm Changwoo, Kim Jongmin, Kim Chohui, Kang Suji, Hwang Taehyun, et al. Review paper: toward highly efficient quantum-dot- and dye-sensitized solar cells. J Curr Appl Phys 2013;13:S2eS13.
[17] Vogel R, Pohl K, Weller H. Sensitization of highly porous, polycrystalline TiO_2 electrodes by quantum sized CdS. J Chem Phys Lett 1990;174:241–6.
[18] Vogel R, Hoyer P, Weller H. Quantum-sized Pbs,Cds,Ag_2S, Sb_2S_3 and Bi_2S_3 particles as sensitizers for various nanoporous wide-bandgap semiconductors. J Phys Chem 1994;98:3183–8.
[19] Ruhle Sven, Shalom Menny, Zaban Arie. Quantum-dot-sensitized solar cells. J Chem Phys Chem 2010;11:2290–304.
[20] Zhou Zhengji, Yuan Shengjie, Fan Junqi, Hou Zeliang, Zhou Wenhui, Du Zuliang, et al. $CuInS_2$ Quantum dot-sensitized TiO_2 nanorod array photoelectrodes: synthesis and performance optimization. J Nanoscale Res Lett 2012;7:652.
[21] Zhu Guang, Xu Tao, Lv Tian, Pan Likun, Zhao Qingfei, Sun Zhuo. Graphene incorporated nanocrystalline TiO_2 films for CdS quantum dot-sensitized solar cells. J Electroanal Chem 2011;650:248–51.
[22] Nazeeruddin MK, Kay A, Rodicio 1, Humpbry-Baker R, Miiller E, Liska P, et al. Conversion of light to electricity by cis-X_2Bis (2,2/-bipyridyl-4 4/dicarboxylate) ruthenium (II) charge-transfer sensitizers (X=C1-, Br-, I-, CN-, and SCN-) on nano crystalline TiO_2 electrodes. J Am Chem Soc 1993;115:6382–90.
[23] Jung Sung Woo, Kim Jae-Hong, Kim Hyunsoo, Choi Chel-Jong, Ahn Kwang-Soon. ZnS over layer on in situ chemical bath deposited CdS quantum dot-assembled TiO_2 films for quantum dot-sensitized solar cells. J Curr Appl Phys 2012;12(6):1459–64.
[24] Kim Jongmin, Choi Hongsik, Nahm Changwoo, Kim Chohui, Nam Seunghoon, Kang Suji, et al. The role of a $TiCl_4$ treatment on the performance of CdS quantum-dot-sensitized solar cells. J Power Sources 2012;220:108–13.
[25] Kongkanand Anusorn, Tvrdy Kevin, Takechi Kensuke, Kuno Masaru, Kamat Prashant V. Quantum dot solar cells. Tuning photoresponse through size and shape control of CdSe–TiO_2 architecture. J Am Chem Soc 2008;130(12):4007–15.
[26] Chi Ching-Fa, Cho Hsun-Wei, Teng Hsisheng, Chuang Cho-Ying, Chang Yu-Ming, Hsu Yao-Jane, et al. Energy level alignment, electron injection, and charge recombination characteristics in CdS/CdSe co-sensitized TiO_2 photoelectrode. J Appl Phys Lett 2011;98:012101.
[27] Chen J, Lei W, Deng WQ. Reduced Charge recombination in a co-sensitized quantum dot solar cell with two different sizes of CdSe quantum dot. J Nanoscale 2011:674–7.
[28] Prabakar K, Minkyu S, Inyoung S, Heeje K. CdSe quantum dots co-sensitized TiO_2 photoelectrodes: particle size dependent properties. J Phys D: Appl Phys 2010;43:012002.
[29] Balis Nikolaos, Dracopoulos Vassilios, Bourikas Kyriakos, Lianos Panagiotis. Quantum dot sensitized solar cells based on an optimized combination of ZnS, CdS and CdSe with CoS and CuS counter electrodes. Electrochim Acta 2013;91:246–52.
[30] Hara Kohjiro, Mori Shogo. Handbook of photovoltaic science and engineering. In: Luque Antonio, Hegedus Steven, editors. Dye-sesitized solar cell. 2nd ed.. . p. 642–74.
[31] Gong Jiawei, Liang Jing, Sumathy K. Review on dye-sensitized solar cells (DSSCs): fundamental concepts and novel materials. Renew Sustain Energy Rev 2012;16:5848–60.
[32] Lee L, Lo Y-S. Highly efficient quantum-dot-sensitized solar cell based on co-sensitization of CdS/CdSe. J Adv Funct Mater 2009;604:19.
[33] Lee YL, Chang C-H. Efficient polysulfide electrolyte for CdS quantum dot-sensitized solar cells. J Power Sources 2008;185:584–8.
[34] Yang Z, Chen C-Y, Roy P, Chang H-T. Quantum dot-sensitized solar cells incorporating nanomaterials. Chem Commun 2011;47:9561–71.
[35] Chiba A Islam, Watanabe Y, Komiya R, Koide N, Han L. Dye-sensitized solar cells with conversion efficiency of 11.1%. J Appl Phys 2006;45:L638–40.
[36] Fukui Atsushi, Fuke Nobuhiro, Komiya Ryoichi, Koide Naoki, Yamanaka Ryohsuke, Katayama Hiroyuki, et al. Dye-sensitized photovoltaic module with conversion efficiency of 8.4%. J Appl Phys 2009;2(8):082202.
[37] El Chaar L, lamonta LA, El Zein N. Review of photovoltaic technologies. Renew Sustain Energy Rev 2011;15:2165–75.
[38] Fuke N, Hoch LB, Koposov AY, Manner VW, Werder DJ, Fukui A, et al. CdSe quantum-dot-sensitized solar cell with 100% internal quantum efficiency. ACS Nano 2010;4:6377–86.

[39] Hishikawa Yoshihiro, Yanagida Masatoshi, Koide Naoki. Characterization of the dye-sensitized solar cells. In: Proceedings of the IEEE photovoltaic specialists conference; 2005. p. 67–70.
[40] Williams KJ, Nelson CA, Yan X, Li LS, Zhu X. Hot electron injection from graphene quantum dots to TiO_2. J ACS Nano 2013;26:1388–94.
[41] Beard Matthew C. Multiple exciton generation in semiconductor quantum dots. J Phys Chem Lett 2011;2:1282–8.
[42] Etgar Lioz. Semiconductor nanocrystals as light harvesters in solar cells. J Mater 2013;6:445–59.
[43] Jun HK, Careem MA, Arof AK. Quantum dot-sensitized solar cells – perspective and recent developments: a review of cd chalcogenide quantum dots as sensitizers. Renew Sustain Energy Rev 2013;22:148–67.
[44] Guyot-Sionnest P, Shim M, Matranga C, Hines M. Long-lived quantum-confined infrared transition in CdSe nano-crystal. Phys Rev 1999;60:R2182.
[45] Califano Marco. Giant suppression of auger electron cooling in charged nanocrystals. J Appl Phys Lett 2007;91:172114–7.
[46] Nozik Arthur J. Multiple exciton generation in semiconductor quantum dots. J Chem Phys Lett 2008;457:3–11.
[47] Ellingson RJ, Beard MC, Johnson JC, Yu P, Micic OI, Nozik AJ, et al. Highly efficient multiple exciton generation in colloidal PbSe and PbS quantum dots. Nano Lett 2005;5(5):865–71.
[48] Schaller Richard D, Pietryga Jeffrey M, Klimov Victor I. Carrier multiplication in InAs nanocrystal quantum dots with an onset defined by the energy conservation limit. Nano Lett 2007;7(11):3469–76.
[49] Ben-Lulu M, Mocatta D, Bonn M, Banin U, Ruhman S. On the absence of detectable carrier multiplication in a transient absorption study of InAs/CdSe/ZnSe core/Shell1/Shell2 quantum dots. Nano Lett 2008;8:1207–11.
[50] Robel I, Subramanian V, Kuno M, Kamat PV. Quantum dot solar cells. Harvesting light energy with CdSe nanocrystals molecularly linked to mesoscopic TiO_2 Films. J Am Chem Soc 2006;128:2385.
[51] Chakrapani V, Tvrdy K, Kamat PV. Modulation of electron injection in CdSe–TiO_2 system through medium alkanility. J Am Chem Soc 2010;132:1228–9.
[52] Shen Q, Guijarro N, Gimenez S, Mora-Sero I, Bisquert J, Lana-Villarreal T, et al. Ultrafast electron and hole dynamics in CdSe quantum dot sensitized solar cells. J Phys Chem C 2010;114:22352.
[53] Li Yafeng, Pang Aiying, Zheng Xiangzhen, Wei Mingdeng. CdS quantum-dot-sensitized Zn_2SnO_4 solar cell. Electrochim Acta 2011;56:4902–6.
[54] Tubtimtae Auttasit, Lee Ming-Way, Wang Gou-Jen. Ag_2Se quantum-dot sensitized solar cells for full solar spectrum light harvesting. J Power Sources 2011;196:6603–8.
[55] Wang X, Koleilat GI, Tang J, Liu H, Kramer IJ, Debnath R, et al. Tandem colloidal quantum dot solar cells employing a graded recombination layer. J Nat Photon 2011;5:480–4.
[56] Gorer S, Hodes G. Quantum size effects in the study of chemical solution deposition mechanism of semiconductor films. J Phys Chem 1994;98:5338–46.
[57] Emin S, Singh SP, Han L, Satoh N, Islam A. Colloidal quantum dot solar cells. Sol Energy 2011;85:1264–82.
[58] Halim MA. Review harnessing Sun's energy with quantum dots based next generation solar cell. Nanomaterials 2013;3:22–47.
[59] Choi Youngwoo, Seol Minsu, Kim Wooseok, Yong Kijung. Chemical bath deposition of stoichiometric CdSe quantum dots for efficient quantum-dot-sensitized solar cell application. J Phys Chem C 2014;118:5664–70.
[60] Hu Y, Wang B, Zhang J, Wang T, Liu R, Zhang J, et al. Synthesis and photoelectrochemical response of CdS quantum dot-sensitized TiO_2 nanorod array photoelectrodes. Nanoscale Res Lett 2013;8:222.
[61] Senthamilselvi V, Saravanakumar K, Begum NJ, Anandhi R, Ravichandran AT, Sakthivel B, et al. Photovoltaic properties of nanocrystalline CdS films deposited by SILAR and CBD techniques – a comparative study. J Mater Sci: Mater Electron 2012;23:302–8.
[62] Gimenez S, Mora-Sero I, Macor L, Guijarro N, Lana-Villarreal T, Go´mez R, et al. Improving the performance of colloidal quantum-dot-sensitized solar cells. Nanotechnology 2009;20:295204.
[63] Guijarro N, Lana-Villarreal T, Mora-Sero I, Bisquert J, Go´mez R. CdSe quantum dot-sensitized TiO_2 electrodes: effect of quantum dot coverage and mode of attachment. J Phys Chem C 2009;113:4208–14.
[64] Mali Sawanta S, Desai Shital K, Kalagi Smita S, Betty Chirayath A, Bhosale Popatrao N, Devan Rupesh S, et al. PbS quantum dot sensitized anatase TiO_2 Nanocorals for quantum dot-sensitized solar cell applications. Dalton Trans 2012;41:6130.
[65] Jiao Jie, Zhou Zheng-Ji, Zhou Wen-Hui, Wu Si-Xin. CdS and PbS quantum dots co sensitized TiO_2 nanorod arrays with improved performance for solar cells application. Mater Sci Semicond Process 2013;16(2):435–40.
[66] Chen Lung-Chuan, Ho Yi-Ching, Yangb Ru-Yuan, Chen Jean-Hong, Huang Chao-Ming. Electro deposited $AgInSe_2$ onto TiO_2 films for semiconductor-sensitized solar cell application: the influence of electrodeposited time. J Appl Surf Sci 2012;58:6558–63.
[67] Benehkohal Nima Parsi, Gonzlez-Pedro Victoria, Boix Pablo P, Chavhan Sudam, Tena-Zaera Ramon, Demopoulos George P, et al. Colloidal PbS and PbSeS quantum dot sensitized solar cells prepared by electrophoretic deposition. J Phys Chem 2012;1(16):16391–7.
[68] Zhang Quanxin, Zhang Yiduo, Huang Shuqing, Huang Xiaoming, Luo Yanhong, Meng Qingbo, et al. Application of carbon counter electrode on CdS quantum dot-sensitized solar cells (QDSSCs). Electrochem Commun 2010;12:327–30.
[69] Gonzalez- Pedro Victoria, Xu Xueqing, Mora-Sero Ivan, Bisquert Juan. Modeling high-efficiency quantum dot sensitized solar cells. ACS Nano 2010;4(10):5783–90.
[70] Yang Zusing, Chang Huan-Tsung. CdHgTe and CdTe quantum dot solar cells displaying an energy conversion efficiency exceeding 2%. Sol Energy Mater Sol Cells 2010;94:2046–51.
[71] Yu X-Y, Lei B-X, Kuang D-B, Su C-Y. High performance and reduced charge recombination of CdSe/CdS quantum dot-sensitized solar cells. J Mater Chem 2012;22:12058–63.
[72] Hu Xing, Zhang Quanxin, Huang Xiaoming, Li Dongmei, Luo Yanhong, Meng Qingbo. Aqueous colloidal $CuInS_2$ for quantum dot sensitized solar cells. J Mater Chem 2011;21:15903.
[73] Fan S-Q, Cao R-J, Xi Y-X, Gao M, Wang M-D, Kima D-H, et al. CdSe quantum dots as co-sensitizers of organic dyes in solar cells for red-shifted light harvesting. J Optoelectron Adv Mater – Rap Commun 2009;10:1027–33.
[74] Karageorgopoulos Dimitrios, Stathatos Elias, Vitoratos Evangelos. Thin ZnO nanocrystalline films for efficient quasi-solid state electrolyte quantum dot sensitized solar cells. J Power Sources 2012;219:9–15.
[75] Li Yafeng, Guo Binbin, Zheng Xiangzhen, Pang Aiying, Wei Mingdeng. Improving the efficiency of CdS quantum dot-sensitized Zn_2SnO_4 Solar cells by surface treatment with Al^{3+} ions. Electrochim Acta 2012;60:66–70.
[76] Bora Tanujjal, Kyaw Htet H, Dutta Joydeep. Zinc oxide–zinc stannate core–shell nanorod arrays for CdS quantum dot sensitized solar cells. Electrochim Acta 2012;68:141–5.
[77] Seo Hyunwoong, Wanga Yuting, Uchida Giichiro, Kamataki Kunihiro, Itagaki Naho, Koga Kazunori, et al. The reduction of charge recombination and performance enhancement by the surface modification of Si quantum dot-sensitized solar cell. Electrochim Acta 2013;87:213–7.
[78] Shu Ting, Xiang Peng, Zhou Zi-Ming, Wang Heng, Liu Guang-Hui, Han Hong-Wei, et al. Mesoscopic nitrogen-doped TiO_2 spheres for quantum dot-sensitized solar cells. Electrochim Acta 2012;68:166–71.
[79] Jang Wonho, Budi Nursanto Eduardus, Kim Jaehoon, Jin Park Se, Koun Min Byoung, Yoo Ki-pung. Liquid carbon dioxide coating of CdS quantum-dots on mesoporous TiO_2 film for sensitized solar cell applications. J Supercrit Fluids 2012;70:40–7.
[80] Xiaoping Zhang, Zhang Lan, Jihuai Wu, Jianming Lin, Leqing Fan. Enhancing photovoltaic performance of photo electro chemical solar cells with nano-sized ultra thin Sb_2S_3-sensitized layers in photoactive electrodes. J Mater Sci: Mater Electron 2013;24:1970–5.
[81] Uchida Giichiro, Yamamoto Kosuke, Sato Muneharu, Kawashima Yuki, Nakahara Kenta, Kamataki Kunihiro, et al. Effect of nitridation of Si nanoparticles on the performance of quantum-dot sensitized solar cells. Jpn J Appl Phys 2012;51:01AD01.
[82] Ning Zhijun, Tian Haining, Yuan Chunze, Fu Ying, Qin Haiyan, Sun Licheng, et al. Solar cells sensitized with type-II ZnSe–CdS core/shell colloidal quantum dots. Chem Commun 2011;47:1536–8.
[83] Chen Jing, Lei Wei, Li Chi, Zhang Yan, Cui Yiping, Wang Baoping, et al. Flexible quantum dot sensitized solar cell by electrophoretic deposition of CdSe quantum dots on ZnO nanorods. J Chem Phys 2011;13:13182–4.
[84] Zhao Junchang, Wu Jihuai, Fuda Yu, Zhang Xiaoping, Lan Zhang, Lin Jianming. Improving the photovoltaic performance of cadmium sulfide quantum dots-sensitized solar cell by graphene/titania photoanode. Electrochim Acta 2013;96:110–6.
[85] Chang Haixin, Lv Xiaojun, Zhang Hao, Li Jinghong. Quantum dots sensitized graphene: in situ growth and application in photo electron chemical cells. Electrochem Commun 2010;12:483–7.
[86] Lee Wonjoo, Lee Jungwoo, Ki Min Sun, Park Taehee, Yi Whikun, Han Sung-Hwan. Effect of single-walled carbon nanotube in PbS/TiO_2 quantum dots-sensitized solar cells. Mater Sci Eng 2009;156:48–51.
[87] Chen J, Li C, Zhao DW, Lei W, Zhang Y, Cole MT, et al. A quantum dot sensitized solar cell based on vertically aligned carbon nanotubes templated ZnO arrays. Electrochem Commun 2010;12:1432–5.
[88] Wang Qing, Zhang Xiaonan, Huo Xiaodi, Zhang Renhui, Dai Jianfeng. Study of nanocrystalline ZnO and Zn_2TiO_4 film electrode with ZnPc dye and PbS quantum dots composite sensitization. Adv Mater Res 2011;287–290:2217–20.
[89] Zhu Guang, Pan Likun, Xu Tao, Zhao Qingfei, Sun Zhuo. Cascade structure of TiO_2/ZnO/CdS film for quantum dot sensitized solar cells. J Alloys Compd 2011;509:7814–8.
[90] Nozik AJ, Beard MC, Luther JM, Law M, Ellingson RJ, Johnson JC. Semiconductor quantum dots and quantum dot arrays and applications of multiple exciton generation to third-generation photovoltaic solar cells. Am Chem Soc Rev 2010;110:6873–90.
[91] Bach Gerd. Single QDs fundamentals, applications, and new concepts. In: Michler Peter, editor. Optical properties of epitaxially grown wide bandgap single quantum dots. New York: Springer; 2003. p. 147–84.
[92] Haining Chen, Weiping Li, Huicong Liu, Liqun Zhu. CdS quantum dots sensitized single- and multi-layer porous ZnO nanosheets for quantum dots-sensitized solar cells. Electrochem Commun 2011;13: 331–334.
[93] Quanxin Z, Xiaozhi G, Xiaoming H, Shuqing H, Dongmei L, Yanhong L, et al. Highly efficient CdS/CdSe-sensitized solar cells controlled by the structural properties of compact porous TiO_2 photo electrodes. Phys Chem Chem Phys 2011;13:4659.
[94] Semonin OE, Luther JM, Choi S, Chen HY, Gao JB, Nozik AJ, et al. Peak external photocurrent quantum efficiency exceeding 100% via MEG in quantum dot solar cell. Science 2011;334(6062):1530–3.

[95] Luther JM, Gao JB, Lloyd MT, Semonin OE, Beard MC, Nozik AJ. Stability assessment on 3% PbS/ZnO quantumquantum dot heterojunction solar cell. Adv Mater 2010;22:3704–7.
[96] Wadia C, Alivisatos AP, Kammen DM. Materials availability expands the opportunity for large-scale photovoltaics deployment. Environ Sci Technol 2009;43:2072–7.
[97] Alexandar H, Susanna M, Hoogland S, Voznyy O, Zhitomirsky D, Debnath R, et al. Hybrid passivated colloidal quantum dot solids. Nat Nanotechnol 2012;**7**:577–82.